THE JOURNAL OF BIOLOGICAL CHEMISTRY VOL. 285, NO. 10, pp. 6913–6921, March 5, 2010

RANKL-mediated Reactive Oxygen Species Pathway That Induces Long Lasting Ca^{2+} Oscillations Essential for Osteoclastogenesis*

Received for publication, August 3, 2009, and in revised form, November 26, 2009 Published, JBC Papers in Press, January 4, 2010, DOI 10.1074/jbc.M109.051557

Min Seuk Kim[‡], Yu-Mi Yang[‡], Aran Son[‡], Yu Shun Tian[‡], Syng-Ill Lee[‡], Sang Won Kang[§], Shmuel Muallem[¶], and Dong Min Shin[‡1]

From the [‡]Department of Oral Biology, Brain Korea 21 Project, Oral Science Research Center, Center for Natural Defense System, Yonsei University College of Dentistry, Seoul 120-752, Korea, the [§]Division of Molecular Life Sciences and the Center for Cell Signaling Research, Ewha Womans University, Seoul 120-750, Korea, and the [¶]Department of Physiology, University of Texas Southwestern Medical Center, Dallas, Texas 75390-9040

RANKL (receptor activator of NF-κB ligand) induces osteoclastogenesis by activating multiple signaling pathways in osteoclast precursor cells, chief among which is induction of long lasting oscillations in the intracellular concentration of Ca^{2+} ($[Ca^{2+}]_i$). The $[Ca^{2+}]_i$ oscillations activate calcineurin, which activates the transcription factor NFATc1. The pathway by which RANKL induces $[Ca^{2+}]_i$ oscillations and osteoclastogenesis is poorly understood. Here we report the discovery of a novel pathway induced by RANKL to cause a long lasting increase in reactive oxygen species (ROS) and $[Ca^{2+}]_i$ oscillations that is essential for differentiation of bone marrow-derived monocytes into osteoclasts. The pathway includes RANKL-mediated stimulation of Rac1 to generate ROS, which stimulate phospholipase Cγ1 to evoke $[Ca^{2+}]_i$ oscillations by stimulating Ca^{2+} release from the inositol 1,4,5-trisphosphate pool and STIM1-regulated Ca^{2+} influx. Induction and activation of the pathway is observed only after 24-h stimulation with RANKL and lasts for at least 3 days. The physiological role of the pathway is demonstrated in mice with deletion of the *Peroxiredoxin II* gene and results in a mark increase is ROS and, consequently, a decrease in bone density. Moreover, bone marrow-derived monocytes in $PrxII^{-/-}$ primary culture show increased ROS and spontaneous $[Ca^{2+}]_i$ oscillations. These findings identify the primary RANKL-stimulated pathway to trigger the late stages of osteoclastogenesis and regulate bone resorption.

Bone is a dynamic tissue that is constantly being remodeled. The remodeling process is a delicate balance between the activities of osteoblasts and osteoclasts. Interference with this balance results in serious human pathologies that affect bone integrity. Tipping the balance in favor of osteoclasts leads to pathological bone resorption, which is observed in autoimmune arthritis, osteoporosis, and periodontitis (1, 2).

Bone marrow-derived monocyte/macrophage precursor cells (BMM)[2] of a hematopoietic origin develop into osteoclasts through cell-to-cell signaling with mesenchymal cells, such as osteoblasts (3, 4). Cell-to-cell interaction between the osteoclast precursors and osteoblastic/stromal cells are also essential for the differentiation of osteoclast progenitor cells into mature osteoclasts (5, 6). RANKL (receptor activator of NF-κB ligand) is expressed in osteoblastic/stromal cells and is vital for osteoclast differentiation (7–11). Stimulation of the RANK receptor by RANKL in the presence of the macrophage colony-stimulating factor (M-CSF) causes osteoclast differentiation and activation *in vitro* (6, 8, 12). Moreover, the binding of RANKL to its receptor results in the recruitment of the TNF receptor-associated factor (TRAF) family of proteins, *e.g.* TRAF6, which are linked to the NF-κB and JNK pathways (13–15). Of particular importance, a series of signals following RANK activation induce oscillations in the free intracellular concentration of Ca^{2+} ($[Ca^{2+}]_i$), which trigger the late stage of osteoclast differentiation by activating the nuclear factor of activated T cells type c1 (NFATc1) (16). Unique aspects of these RANKL-stimulated Ca^{2+} oscillations is that they are observed only 24–48 h post-stimulation, indicating the need for induction of the pathway responsible for the Ca^{2+} oscillations. The nature of this pathway and how it is induced are not known.

Ca^{2+} is a ubiquitous intracellular messenger that mediates a wide variety of cellular functions and is involved in the fundamental cellular processes of proliferation, differentiation, and programmed cell death (17). In the case of osteoclast differentiation, Ca^{2+} plays an important role by sequentially activating calcineurin and NFATc1 (16). Members of the NFAT family are among the most strongly induced transcription factors following RANKL stimulation. During osteoclastogenesis, costimulatory signals mediated by the immunoreceptor tyrosine-based

* This work was supported by Grant A084007 from the Korea Healthcare Technology R & D Project, Ministry for Health, Welfare and Family Affairs, Republic of Korea.

[1] To whom correspondence should be addressed: Dept. of Oral Biology, Yonsei University College of Dentistry, 134 Shinchon-dong, Seodaemon-gu, Seoul 120-752, Korea. Tel.: 82-2-2228-3051; Fax: 82-2-364-1085; E-mail: dmshin@yuhs.ac.

[2] The abbreviations used are: BMM, bone marrow-derived monocyte; ROS, reactive oxygen species; PLC, phospholipase C; RANKL, receptor activator of NF-κB ligand; STIM1, stromal interacting molecule 1; IP_3, inositol 1,4,5-trisphosphate; M-CSF, macrophage colony-stimulating factor; TNF, tumor necrosis factor; TRAF, TNF receptor-associated factor; JNK, Jun N-terminal kinase; NFAT, nuclear factor of activated T cells; SOC, store-operated Ca^{2+} influx channel; Xest C, xestospongin C′; DPI, diphenylene iodonium; NAC, *N*-acetyl-L-cysteine; siRNA, small interfering RNA; TRAP, tartrate-resistant acid phosphatase; WT, wild type; DN, dominant negative; ER, endoplasmic reticulum; TRP, transient receptor.

activation motif and the activation of phospholipase Cγ1 (PLCγ1) are involved in RANKL-induced $[Ca^{2+}]_i$ oscillations and activation of NFATc1 (18). The tyrosine kinases Btk and Tec are also involved in the activation of PLCγ1 by linking the RANK and immunoreceptor tyrosine-based activation motif signals (19). However, the signals upstream and downstream of PLCγ1 that are stimulated by RANKL to generate $[Ca^{2+}]_i$ oscillations and the mechanism for generation of the $[Ca^{2+}]_i$ oscillations are not known.

We report here the discovery of a novel redox pathway activated by RANKL that is upstream of PLCγ1 and is essential for RANKL-induced $[Ca^{2+}]_i$ oscillations and osteoclastogenesis. This study originated with the observation that mice with knock-out of peroxiredoxin II (PrxII), a thiol-based peroxide reductase that clears cellular H_2O_2, develop severe bone loss and osteoporosis. We were able to track the phenotype to altered long term RANKL-generated reactive oxygen species (ROS) and consequently osteoclast differentiation. ROS, including the superoxide anion ($O_2^{\cdot-}$) and H_2O_2, are well recognized second messengers that participate in a variety of cellular functions (20). Through the use of BMMs in wild type and PrxII knock-out mice and through genetic and pharmacological manipulation of Rac1, PrxII, PLCγ1, Ca^{2+} release from stores, and the store-operated Ca^{2+} influx channel (SOC) regulator stromal interacting molecule 1 (STIM1), we identified the pathway induced by RANKL to generate Ca^{2+} oscillations and regulate osteoclastogenesis and bone metabolism.

EXPERIMENTAL PROCEDURES

Cell Culture and Reagents—RAW264.7 (Korean Cell Line Bank, South Korea) and primary cultured BMMs were maintained in Dulbecco's modified Eagle's medium (Invitrogen) and α-minimum essential medium supplemented with 10% fetal bovine serum (Invitrogen) and incubated in 5% CO_2. To maintain BMMs, α-minimum essential medium was supplemented with 50 ng/ml M-CSF. Receptor activator of RANKL and M-CSF were purchased from KOMA Biotech (South Korea). Fura-2/AM was purchased from Teflabs (Austin, TX). Xestospongin C (Xest C), gadolinium chloride (Gd^{3+}), U73122, U73343, 2′,7′-dichlorofluorescein diacetate, diphenylene iodonium (DPI), and *N*-acetyl-L-cysteine (NAC) were from Sigma-Aldrich. The STIM1–1140 RNA interference and scramble RNA interference were purchased from Dharmacon (Thermo Fisher Scientific, Lafayette, CO). Polyclonal antibody for phospho-PLCγ1 (p-PLCγ1, Tyr^{783}) was from Millipore (Billerica, MA). Monoclonal antibodies for NFATc1 and plasma membrane Ca^{2+} ATPase (PMCA-5F10) were obtained from Santa Cruz Biotechnology (Santa Cruz, CA) and Affinity Bioreagents (Golden, CO), respectively. Monoclonal antibodies for PLCγ1 and p-SUPER-PLCγ1 siRNA were generous gifts from Dr. Yun Soo Bae (Ewha University, Seoul, South Korea). The $PrxII^{-/-}$ mice (21) were provided by Dr. Sang Won Kang (Ewha University).

Preparation of BMMs—The femur and tibia were removed from 4–6-week-old mice. The cells derived from the bone marrow of femur and tibia were collected and cultured in α-minimum essential medium containing 10% fetal bovine serum and 10 ng/ml M-CSF. The following day, nonadherent cells were collected and seeded in 6-well plates and treated with M-CSF (50 ng/ml). After 2 days the nonadherent cells were washed out, and the adherent cells were used as BMMs.

DNA/siRNA Transfection—Approximately $1–5 \times 10^5$ cells were seeded on a 35-mm dish and incubated in antibiotic-free medium, and after 24 h, the cells were replated. Plasmids in 250 μl of Lipofectamine 2000 (Invitrogen) were diluted with 250 μl of Opti-MEM. The mixtures were incubated for 20 min at room temperature before adding the cell. siRNA-transfected cells were assayed by reverse transcription-PCR and compared with cells transfected with scrambled siRNA. Green fluorescent protein-positive cells were identified and used for $[Ca^{2+}]_i$ measurements.

$[Ca^{2+}]_i$ Measurement—The cells were seeded on cover glass in a 35-mm dish (5×10^4 cells/coverslip) and stimulated with RANKL (50 ng/ml) for the indicated times. When necessary, cells were pretreated with the required agents (U73122, U73343, Xest C, Gd^{3+}, NAC, and DPI), and the agents were also included in the perfusate. The cells were incubated with 5 μM Fura-2/AM for 40 min at room temperature and washed with bath solution (140 mM NaCl, 5 mM KCl, 1 mM $MgCl_2$, 10 mM HEPES, 1 mM $CaCl_2$, 10 mM glucose, 310 mOsm, pH 7.4). The coverslips were transferred to a perfusion chamber, and the cells were continuously perfused with prewarmed (37 °C) bath solution. Fura-2 fluorescence intensity was measured using excitation wavelengths of 340 and 380 nm, and the emitted fluorescence at 510 nm (Ratio = F_{340}/F_{380}) was monitored using a CCD camera (Universal Imaging Co., Downingtown, PA). The images were digitized and analyzed by MetaFluor software (Universal Imaging).

Detection of GTP-bound Rac1—RAW264.7 cells were stimulated with RANKL (50 ng/ml) for the indicated times. The cells were lysed with ice-cold lysis buffer (50 mM Tris, pH 7.4, 100 mM NaCl, 2 mM $MgCl_2$, 10% glycerol, 1% Nonidet P-40, 1 mM dithiothreitol, and protease inhibitor cocktail (Sigma-Aldrich)). Whole cell lysates were then incubated with 10 μg of glutathione *S*-transferase-CRIB (Cdc42 and Rac interaction binding region) overnight at 4 °C. The following day, the cell lysates were centrifuged for 5 min at 13,000 rpm, and the supernatant was incubated with glutathione-Sepharose beads for 2 h at 4 °C. The beads were washed with washing buffer (50 mM Tris, pH 7.4, 100 mM NaCl, 2 mM $MgCl_2$, 10% glycerol, 1% Nonidet P-40, 1 mM dithiothreitol), and the bound proteins were eluted in Laemmli sample buffer and separated by 15% SDS-PAGE. Monoclonal antibody for Rac1 was used to detect GTP-bound Rac1.

TRAP Staining—BMMs were seeded in 48-well plates at a density of 2×10^4 cells/well and pretreated with the indicated compounds. The cells were then stimulated with RANKL (50 ng/ml) supplemented with M-CSF. Six days later osteoclastogenesis was confirmed by TRAP staining. Cytochemical staining of TRAP-positive cells was with the leukocyte acid phosphate assay kit (Sigma-Aldrich), following the manufacturer's procedure. $TRAP^+$ multinucleated (≥3 nuclei) cells were then counted.

Measurement of Intracellular Reactive Oxygen Species—The cells were seeded in 35-mm dishes at a density of 5×10^4. Confluent cells were washed with Hanks' balanced salt solution and incubated for 5 min in the dark at 37 °C in the same solution containing 5 μM 2′,7′-dichlorofluorescin diacetate. The cells

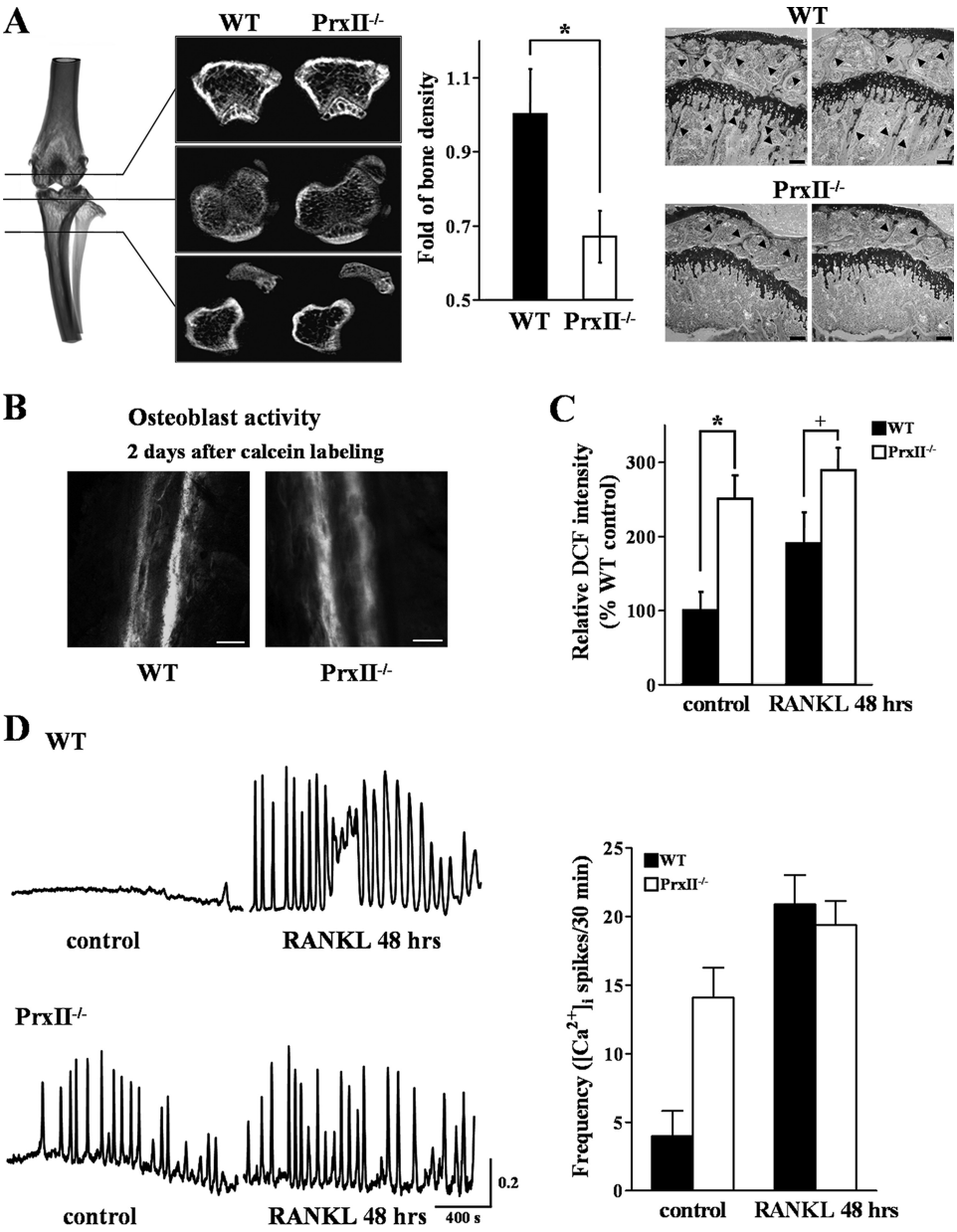

FIGURE 1. **Decreased bone density and increased $[Ca^{2+}]_i$ oscillations in PrxII$^{-/-}$ mice.** *A*, microradiograph and histology (toluidine blue staining; *scale bar*, 50 μm) of tibiae from WT and PrxII$^{-/-}$ mice at 8 weeks of age ($n = 4$). *B*, histological active bone formation of undecalcified tibiae bone from calcein-administered mice (*scale bar*, 20 μm). *C*, measurement of ROS production in WT and PrxII$^{-/-}$ BMMs before and 48 h after RANKL stimulation. *D*, oscillatory change in $[Ca^{2+}]_i$ in WT and PrxII$^{-/-}$ BMMs before and 48 h after RANKL stimulation. The data were normalized to bone volume and ROS production in WT mice and expressed as the means ± S.E. *, $p < 0.01$; +, $p < 0.05$ compared with WT.

were then examined with a laser-scanning confocal microscope (model LSM 510; Carl Zeiss) equipped with an argon laser. Four fields were randomly selected from each sample, and the mean relative fluorescence intensity for each field was measured with a Zeiss vision system and averaged. All of the experiments were repeated at least four times.

Western Blot—Whole cell lysates were prepared by extracting cells with radioimmune precipitation assay lysis buffer (20 mM Tris, pH 7.4, 250 mM NaCl, 2 mM EDTA, pH 8.0, 0.1% Triton X-100, 0.01 mg/ml aprotinin, 5 μg/ml leupeptin, 0.4 mM phenylmethylsulfonyl fluoride, and 4 mM $NaVO_4$), and the extracts were spun at 12,000 rpm for 10 min to remove insoluble material. Cleared extracts (50~100 μg of protein/well) were subjected to 6–12% SDS-PAGE, and the proteins were electrotransferred to a nitrocellulose membrane, blocked with 6% skimmed milk, and probed with antibodies against p-PLCγ1 (1:1000), PLCγ1 (1:3000), and Rac1 (1:1000). The blots were washed, exposed to horseradish peroxidase-conjugated secondary antibodies for 1 h, and detected by chemiluminescence (Amersham Biosciences).

Analysis of Bone Density and Skeletal Morphology—Femur and tibia were removed from WT and PrxII$^{-/-}$ mice. To exclude differences caused by threshold resolution set-up, samples from WT and PrxII$^{-/-}$ were set in one polystyrene holder. Bone density was then measured with a three-dimensional Micro-CT (SkyScan-1076 high resolution *in vivo* micro-CT system; SkyScan, Aartselaar, Belgium) and analyzed with CTAn and Cone beam reconstruction software. Histological examination was performed as described elsewhere (22, 23).

Dynamic Histomorphometry of Bone Formation—Dynamic histomorphometric method was as described before (24) with several modifications. Briefly, 4-week-old male mice were injected twice with calcein (15 mg/kg intraperitoneally) 2 days apart. The animals were sacrificed on day 4, and undeclacified bones were embedded in methyl methacrylate. Longitudinal sections (10-μm thickness) of the tibiae were prepared, and new bone formation was assessed by confocal microscopy of calcein green.

Statistics—The results are expressed as the means ± S.E. from at least three independent experiments. The statistical significances of differences between groups were determined using Student's *t* test (+, $p < 0.05$; *, $p < 0.01$; **, $p < 0.005$).

RESULTS

Spontaneous Increase of ROS in PrxII$^{-/-}$ BMMs Causes Induction of Autonomous $[Ca^{2+}]_i$ Oscillations and a Decrease of Bone Density in PrxII$^{-/-}$ Mice—PrxII is a thiol-based peroxide reductase that clears cellular H_2O_2 and other free radicals to reduce cellular ROS (25). In this study we first examined whether deletion of PrxII alters Ca^{2+} signaling, osteoclasto-

genesis, and bone remodeling and its relation to ROS. To determine the specific role of PrxII in osteoclastogenesis, the tibiae of WT and PrxII$^{-/-}$ mice were dissected, and bone density was measured by microradiographical and histological analyses. The bone density of PrxII$^{-/-}$ tibiae was reduced by ~31% compared with WT tibiae (Fig. 1*A*).

To further analyze the effect of PrxII deletion on bone formation, we performed dynamic histomorphometric measurement on 4-week-old mice injected twice with calcein. Osteoblast function was not influenced by deletion of PrxII, as reported by similar calcein labeling (Fig. 1*B*). To determine the effect of PrxII deletion on ROS and osteoclastogenesis, we measured intracellular ROS in WT and PrxII$^{-/-}$ BMMs. The level of ROS in BMMs from PrxII$^{-/-}$ mice was 2.5-fold higher than in WT BMMs and did not increase further upon 48 h of treatment with RANKL (Fig. 1*C*).

RANKL controls osteoclastogenesis by induction of long lasting Ca^{2+} oscillations that starts ~24–48 h after RANKL treatment (see below and Ref. 16). $[Ca^{2+}]_i$ oscillations in WT cells were observed 48 h after RANKL treatment. By contrast, only spontaneous Ca^{2+} oscillations were observed in PrxII$^{-/-}$ BMM cells, and most importantly, neither the frequency nor the amplitude of the Ca^{2+} oscillations was affected by RANKL stimulation (Fig. 1*D*).

To verify the chronic effects of deleting PrxII on signaling and bone homeostasis observed in the mice and to develop an experimental system to study the molecular characteristics of the pathway linking RANKL, ROS, Ca^{2+} oscillations, and osteoclastogenesis, we determined the effect of overexpressing a dominant negative PrxII (DN-PrxII) in RAW264.7 cells. Fig. 2*A* shows that overexpression of DN-PrxII caused an increase in the steady-state level of ROS and induced $[Ca^{2+}]_i$ oscillations in the absence of RANKL stimulation, as was found

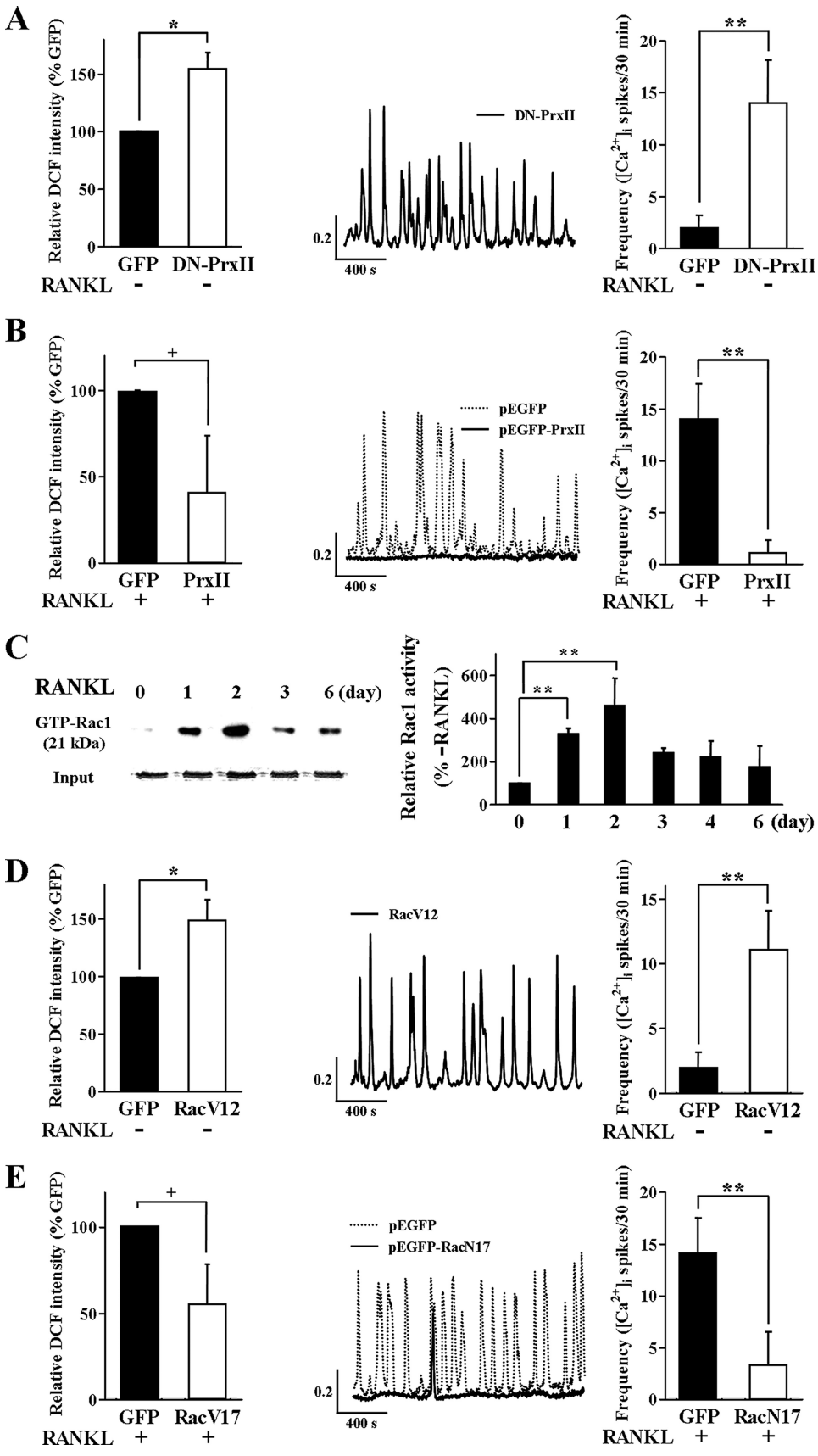

in BMMs obtained from the PrxII$^{-/-}$ mice. On the other hand, overexpression of WT PrxII reduced the RANKL-evoked ROS production and $[Ca^{2+}]_i$ oscillations (Fig. 2*B*). Hence, the *in vitro* system recapitulates the effects observed in the PrxII$^{-/-}$ mice and indicates that deletion of PrxII causes a decrease in bone density by inducing autonomous generation of ROS to induce Ca^{2+} oscillations that are similar to the RANKL-evoked Ca^{2+} oscillations.

To further probe the signaling pathway linking RANKL and ROS to osteoclastogenesis, we tested the role of Rac1, which was reported to function upstream of receptor-mediated ROS generation (26). We assayed the long term activation of Rac1 by RANKL, at the time when RANKL-induced ROS activation and Ca^{2+} oscillations are observed. RANKL-mediated activation of Rac1 is evident after 1 day and peaks after 2 days of stimulation with RANKL (Fig. 2*C*). In parallel, the effect of a constitutively active form of Rac1 (RacV12) was examined to determine whether Rac1 is located upstream of and is involved in the generation of ROS and Ca^{2+} oscillations. Expression of RacV12 resulted in an increased level of ROS production and in spontaneous Ca^{2+} oscillations, equivalent to those induced by RANKL stimulation (Fig. 2*D*). Moreover, the dominant negative form of Rac1 (RacN17) significantly inhibited RANKL-stimulated ROS production and reduced the frequency of the associated Ca^{2+} oscillations (Fig. 2*E*).

RANKL-dependent and -independent Ca^{2+} Oscillations Require the Activation of PLCγ1, IP_3-mediated Ca^{2+} Release and STIM1-regulated Ca^{2+} Influx by SOC Channels—To explore the pathway downstream of ROS that induces the Ca^{2+} oscillations, we examined whether RANKL induces long term activation of PLCγ1 (as revealed by PLCγ1 phosphorylation) and the Ca^{2+} transporting pathways mediating the oscillations. First, we confirmed the phosphorylation of PLCγ1 that was simultaneous with the generation of RANKL-induced Ca^{2+} oscillations. PLCγ1 was phosphorylated after 1 day of RANKL stimulation and remained phosphorylated for at least 2 days (Fig. 3*A*). This is the first demonstration of long term activation of PLCγ1 by RANKL. The essential role of PLCγ1 in RANKL-induced Ca^{2+} oscillations is shown by marked inhibition of the oscillations in cells in which PLCγ1 was knocked down with PLCγ1 siRNA (Fig. 3*B*).

To examine the role of PLCγ1 in RANKL-induced Ca^{2+} oscillations in native cells, we tested the effect of inhibition of PLC activity on the oscillations. Inhibition of PLC activity with the PLC inhibitor U73122 inhibited RANKL-induced Ca^{2+} oscillations in WT BMM cells. The inactive analogue U73343 had no effect (Fig. 3*C*). Importantly, the spontaneous Ca^{2+} oscillations in BMMs from PrxII$^{-/-}$ mice are also inhibited by inhibition of PLC (Fig. 3*C*), indicating that deletion of PrxII resulted in sustained activation of PLC to induce the spontaneous long lasting Ca^{2+} oscillations.

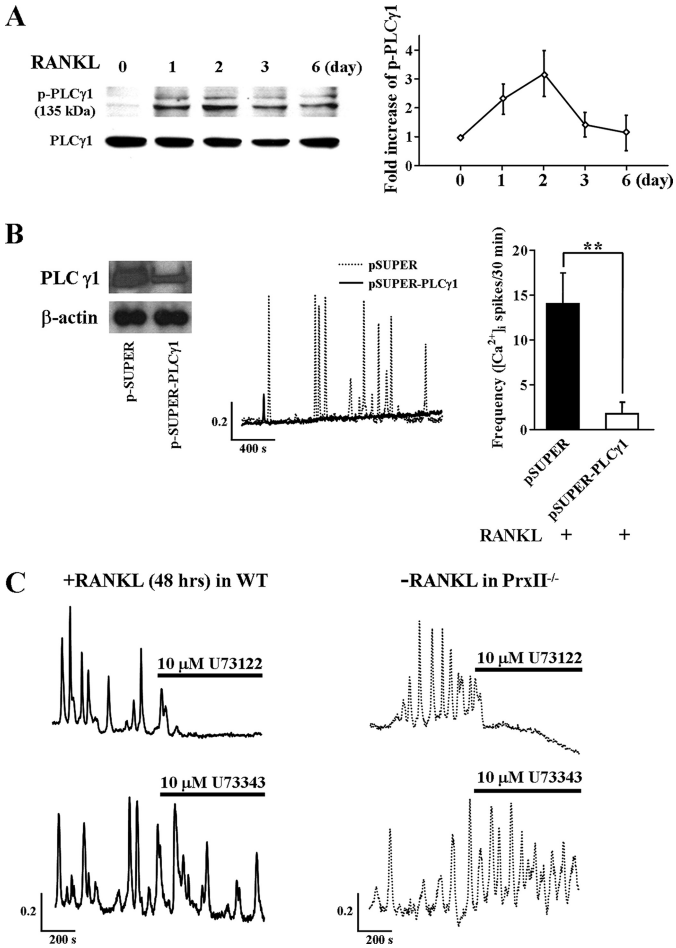

FIGURE 3. **Increased PLCγ1 phosphorylation and role of PLCγ in RANKL-induced $[Ca^{2+}]_i$ oscillations.** *A*, expression level of p-PLCγ1 and total PLCγ1 in BMMs of WT after RANKL stimulation ($n = 4$). *B*, inhibition of RANKL-induced $[Ca^{2+}]_i$ oscillations by knockdown of PLCγ1 ($n = 4$). *C*, inhibitory effect of RANKL-induced and spontaneous $[Ca^{2+}]_i$ oscillations in BMMs from WT and PrxII$^{-/-}$ mice by the PLC inhibitor U73122 and lack of effect by the inactive analogue U73343 ($n = 5$). **, $p < 0.005$ compared with control cells.

RANKL-induced $[Ca^{2+}]_i$ oscillations were examined next. To probe the role of Ca^{2+} release from the endoplasmic reticulum (ER), cells were treated with the IP_3 receptor inhibitor Xest C. Acute inhibition of the IP_3 receptors by 10 μM Xest C eliminated both the RANKL-induced and spontaneous Ca^{2+} oscillations in BMMs from WT and PrxII$^{-/-}$ mice (Fig. 4*A*).

Ca^{2+} oscillations require a continued supply of Ca^{2+} to reload the stores between Ca^{2+} spikes. Potential Ca^{2+} influx channels can be the transient receptor potential (TRP) channels TRPM2 and TRPC3 that were reported to be activated by ROS and nitric oxide, respectively (27, 28). However, reverse transcription-PCR analysis revealed that RAW264.7 cells or BMMs do not express these channels (not shown). Other Ca^{2+} influx channels related to Ca^{2+} oscillations are

FIGURE 2. **Autonomous $[Ca^{2+}]_i$ oscillation by RANKL-independent generation of ROS and Rac1 activation via RANKL signaling pathway.** *A*, effects of DN-PrxII expression on ROS production and $[Ca^{2+}]_i$ oscillations in RAW264.7 cells ($n = 4$). *B*, effects of PrxII overexpression ROS production and $[Ca^{2+}]_i$ oscillations in RAW264.7 cells ($n = 4$). *C*, activation of Rac1 by RANKL in RAW246.7 cells probed with GTP-Rac1 ($n = 5$). *D*, effect of the active form of Rac1 (RacV12) expression on ROS production and $[Ca^{2+}]_i$ oscillations in RAW264.7 cells ($n = 5$). *E*, effects of dominant negative Rac1 (RacN17) expression on ROS production and $[Ca^{2+}]_i$ oscillations in RAW264.7 cells ($n = 5$). The data were normalized to ROS production in control cells transfected with green fluorescent protein (*GFP*) and expressed as the means ± S.E. *, $p < 0.01$; +, $p < 0.05$; **, $p < 0.005$ compared with control cells.

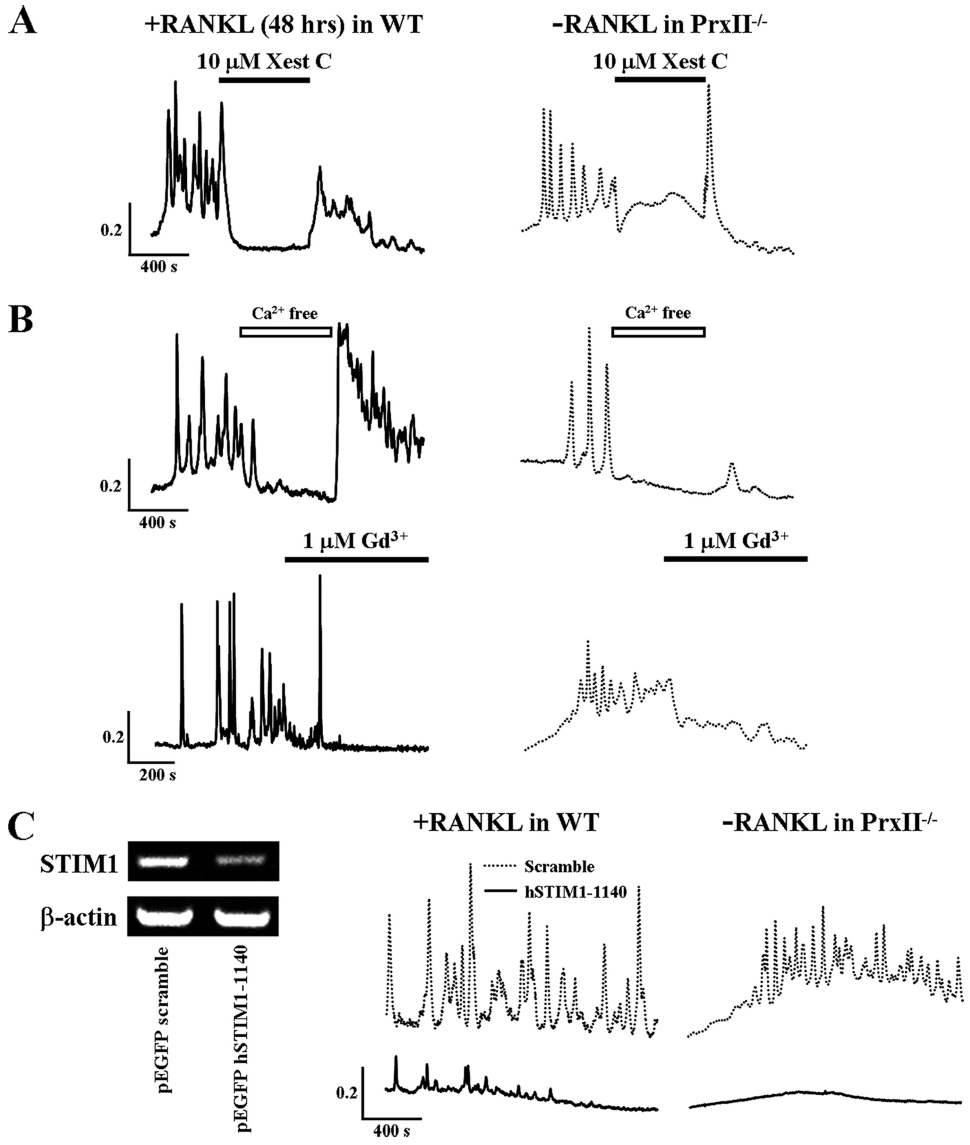

FIGURE 4. **RANKL-induced and spontaneous $[Ca^{2+}]_i$ oscillations depend on Ca^{2+} release from the IP_3 pool and Ca^{2+} influx by SOCs.** *A*, RANKL-induced and spontaneous Ca^{2+} oscillations in WT and PrxII$^{-/-}$ BMM cells are inhibited by inhibition of IP_3-mediated Ca^{2+} release. *B*, dependence of $[Ca^{2+}]_i$ oscillations on extracellular Ca^{2+} in BMMs from WT and PrxII$^{-/-}$ mice ($n = 5$). *C*, knockdown of the ER Ca^{2+} sensor STIM1 inhibits $[Ca^{2+}]_i$ oscillations WT and PrxII$^{-/-}$ BMM cells.

the SOCs, which are activated in response to Ca^{2+} release from the ER (29, 30). Indeed, the removal of extracellular Ca^{2+} and the SOC blocker Gd^{3+} (1 μM) rapidly terminated both types of Ca^{2+} oscillations (Fig. 4*B*). Recent work identified the ER-resident Ca^{2+}-binding protein STIM1 as the ER Ca^{2+} content sensor that conveys the ER Ca^{2+} load to the plasma membrane SOCs (25, 31). In response to Ca^{2+} release from the ER, STIM1 clusters into punctae at the ER/plasma membrane junctions, interacts with the SOCs, and activates them (32, 33). To determine the role STIM1-regulated SOCs in Ca^{2+} oscillations, STIM1 was knocked down with hSTIM1–1140 siRNA. Knockdown of STIM1 attenuated the RANKL-induced Ca^{2+} oscillations in WT BMMs and the spontaneous Ca^{2+} oscillations in PrxII$^{-/-}$ BMMs (Fig. 4*C*).

Long Term ROS Production by RANKL Mediates the Ca^{2+} Oscillations and Regulates Osteoclast Differentiation via PLCγ Activation—Ca^{2+} oscillations appear only after ~1 day of stimulation with RANKL and last for up to 3 days to allow completion of osteoclastogenesis. If production of ROS mediates the oscillations, then RANKL-mediated ROS production must persist for at least 3 days. We examined this prediction by measuring the time course of ROS production in response to RANKL stimulation using 2′,7′-dichlorofluorescein diacetate fluorescence. RANKL-induced ROS production is observed during 3 days of RANKL stimulation (Fig. 5*A*). These results are the first to show that the time course of RANKL-induced ROS production is similar to the time course of RANKL-induced Ca^{2+} oscillations.

To test whether ROS production is required only for induction or also for sustaining the Ca^{2+} oscillations, we determined the effect of inhibiting ROS production at different times before or after RANKL stimulation. The cells were either pretreated with 10 mM of the antioxidant NAC for 30 min before RANKL stimulation or exposed acutely to NAC and to DPI, a NAD(P)H oxidase inhibitor, during the oscillations. No Ca^{2+} response was observed in cells pretreated with NAC (Fig. 5*B*). Moreover, exposing oscillating cells to NAC or DPI inhibited ongoing Ca^{2+} oscillations (Fig. 5*C*), indicating the need for continuous ROS production to sustain the oscillations.

The physiological role of long term ROS production was studied by determining the effect of selective ROS scavenging on activation of PLCγ1 and osteoclast differentiation. To determine whether the production of ROS is directly related to PLCγ1 activation, osteoclast precursor cells were treated with NAC and RANKL for 48 h. Scavenging ROS reduced PLCγ1 phosphorylation by 77 ± 8.3% (Fig. 5*D*). Chronic scavenging of ROS markedly reduced the 1- and 3-day RANKL-induced osteoclast differentiations by 41.9 ± 12%, as revealed by reduction in the formation of multinucleated cells. Importantly, acute ROS scavenging, by 1 h of treatment with NAC had no effect on the formation of multinucleated cells (Fig. 5, *E* and *F*). Hence, the reported acute transient stimulation of ROS production by RANKL (34) is not the ROS that mediates the Ca^{2+} oscillations and osteoclastogenesis. Rather, it is the long term production of ROS that mediates the osteoclastogenesis.

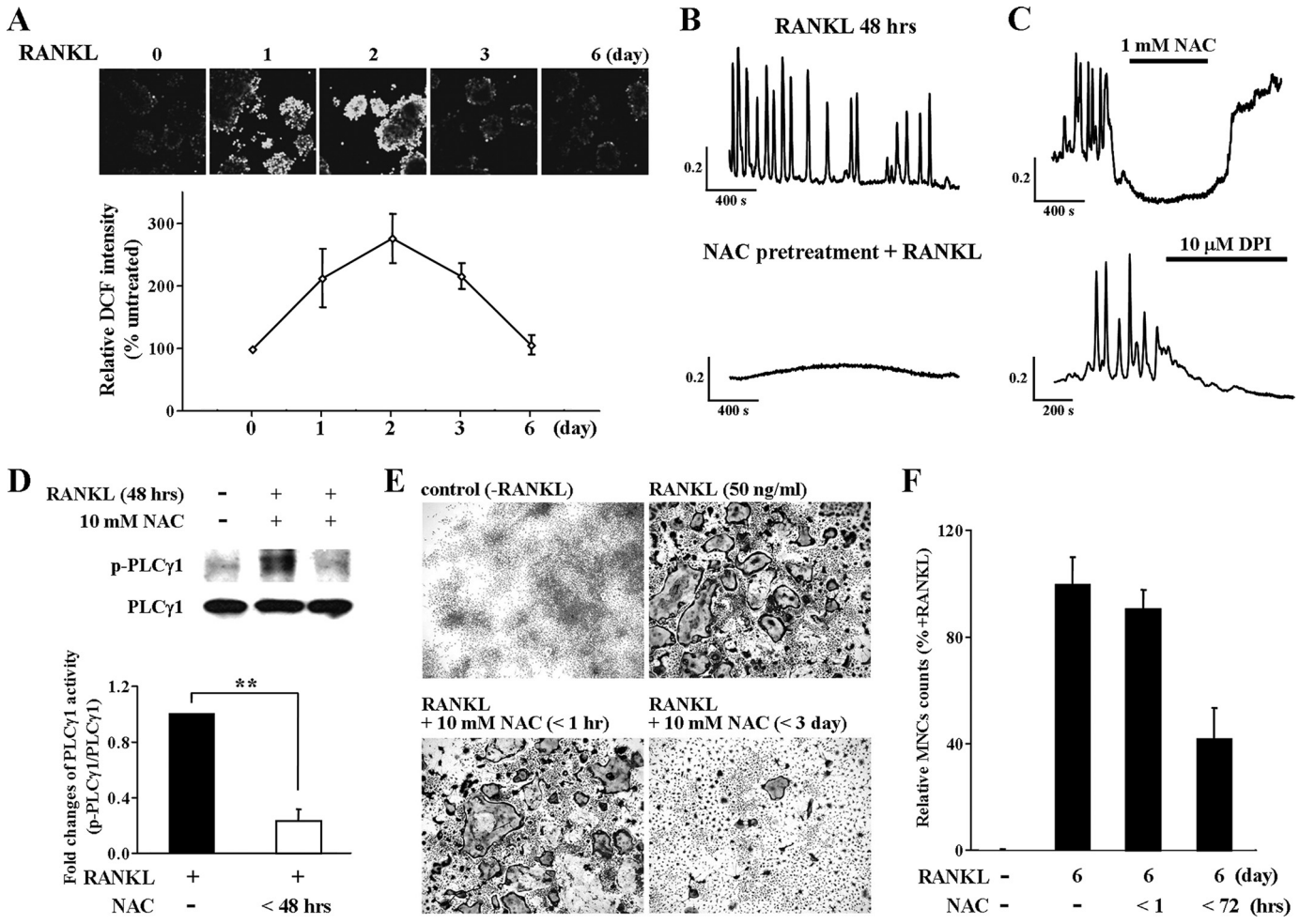

FIGURE 5. **Sustained ROS production by RANKL-induced $[Ca^{2+}]_i$ oscillation and dependence of osteoclastogenesis on PLCγ1.** *A*, measurements of ROS production in RANKL stimulated WT BMMs. The results are expressed as the means ± S.E. ($n = 5$). *B*, inhibition of RANKL-induced $[Ca^{2+}]_i$ oscillations by pretreatment with NAC, an inhibitor of ROS production. *C*, inhibition of RANKL-induced $[Ca^{2+}]_i$ oscillations by NAC and DPI, an inhibitor of NAD(P)H oxidase. *D*, expression levels of p-PLCγ1 and PLCγ1 in WT BMMs in response to RANKL stimulation ($n = 4$). *E* and *F*, RANKL-induced osteoclast differentiation *in vitro* in WT BMMs (TRAP staining) ($n = 4$). **, $p < 0.005$ compared with RANKL-induced PLCγ1 phosphorylation.

DISCUSSION

The RANK-RANKL cytokine system is the chief regulator of osteoclastogenesis. RANKL stimulation activates a series of mediators that are essential for differentiation of precursor mononucleated cells into multinucleated osteoclasts (35). These include activation of the Btk kinase that is associated with activation of PLCγ1, TRAF6, and c-Fos to trigger Ca^{2+} oscillations that activate the calcineurin/NFATc1 transcription system and osteoclastogenesis. However, the signals that are activated by RANKL to activate PLCγ1 and how RANKL induces Ca^{2+} oscillations are not known. RANKL is a member of the TNF receptor family (36). Unique to RANK and other TNF receptor is that they induce Ca^{2+} oscillations only after long stimulation, with the oscillations starting ~24 h post-stimulation and lasting for more than 72 h (16, 18).

We found that RANKL stimulation induces a novel signaling pathway that leads to generation of ROS and Ca^{2+} oscillations and is essential for osteoclastogenesis. The essential components of the pathway are depicted in Fig. 6. Most notably, the components of the pathway are all induced and activated after 24 h of RANKL stimulation and remain activated for 72 h or longer. The most upstream component activated by RANKL identified in the present study is the small G protein Rac1 (Fig. 2*C*). Strikingly, activation of Rac1 was sufficient to induce the long term Ca^{2+} oscillations and ROS production, indicating a central role for Rac1 in RANKL signaling. Rac1 was also reported to be required for the acute generation ROS observed after 10 min of stimulation with epidermal growth factor in epithelial cells (26). Whether the short term and long term effects of Rac1 occur through the same pathway remains to be determined. The long lasting activation of ROS by Rac1 may involve ROS-induced ROS release (37). For example, serum withdrawal was shown to trigger ROS-induced ROS release in human 293T cells. Serum withdrawal leads to an immediate mitochondria response and release ROS, which in turn activates the Rac1/Nox 1 pathway to generate ROS for 4–6 h (38). This requires ROS-induced ROS release. Similarly, our findings of activation of Rac1 by RANKL may mediate activation of Nox1, which transiently generates intracellular ROS (26). This, in turn, is likely to stimulate the mitochondria to cause sustained ROS generation.

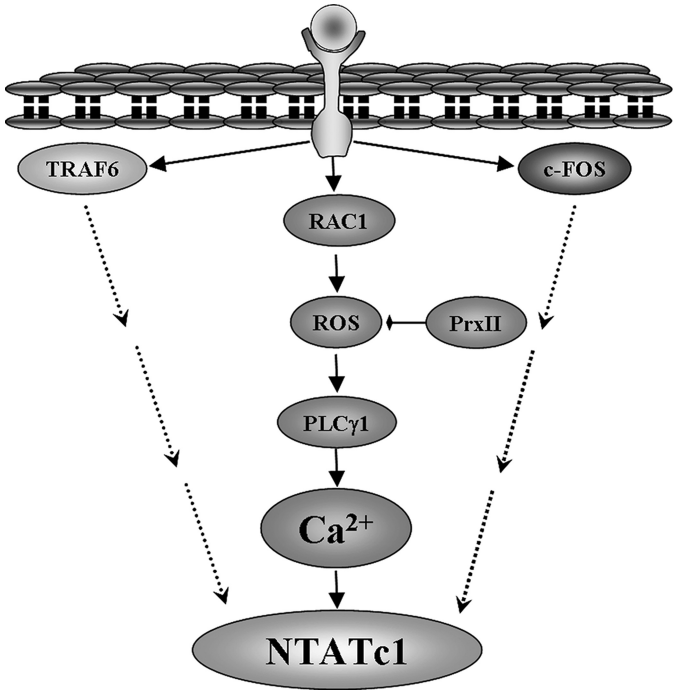

FIGURE 6. **Model depicting the pathway for RANKL-dependent ROS production and osteoclastogenesis.** The model shows the sequence of events activated by RANKL to induce the long term and persistent Ca^{2+} oscillations that are required for the activation of NFATc1. The activation of NFATc1 also requires inputs from direct or indirect RANKL-mediated activation of TRAF6 and c-Fos by yet to be determined mechanism (*dashed arrows*).

By virtue of ROS generation by the constitutively active Rac1, the enzyme that regulates the ROS is downstream of Rac1. We identified this enzyme as PrxII (Figs. 1 and 2). PrxII is a thiol-based peroxide reductase that specifically clears cellular H_2O_2, which indicates that the main ROS generated by RANKL is H_2O_2. Overexpression of PrxII to scavenge the RANKL-generated H_2O_2 eliminated the RANKL-induced Ca^{2+} oscillations. Conversely, expression of dominant negative PrxII increased ROS production and generated spontaneous Ca^{2+} oscillations (Fig. 2*A*). Furthermore, spontaneous Ca^{2+} oscillations are observed in BMMs isolated from the PrxII$^{-/-}$ mice (Fig. 1). The Ca^{2+} oscillations generated by the DN-PrxII and those observed in PrxII$^{-/-}$ BMMs have the same characteristics as the Ca^{2+} oscillations induced by RANKL in WT BMMs and RAW264.7 cells.

In the next step in the pathway, the ROS generated by Rac1 leads to activation of PLCγ1. Indeed, inhibition of RANKL-mediated ROS generation inhibits activation of PLCγ1 (Fig. 5*D*), placing activation of PLCγ1 downstream of ROS generation. Although activation of PLCγ1 by RANKL was reported before (20), the activation was transient and occurred during the first 1 h of RANKL stimulation, long before Ca^{2+} oscillations ensue. The role of the acute activation of PLCγ1 by RANKL is not known at present. Here we show that RANKL stimulation activates PLCγ1 after 24–72 h. The long term activation of PLCγ1 is required for the generation of Ca^{2+} oscillations because knockdown of PLCγ1 almost completely inhibited the RANKL-induced Ca^{2+} oscillations. In addition, the persistent activation of PLCγ1 is required to maintain the oscillations, because inhibition of cellular PLC activity with the pan PLC inhibitor U73122 halted ongoing Ca^{2+} oscillations induced by RANKL (Fig. 3).

The long term and persistent activation of PLCγ1 leads to generation of Ca^{2+} oscillations. The oscillations required Ca^{2+} release from internal stores, as revealed by their inhibition by the IP_3 receptors inhibitor Xest C. Sustaining the Ca^{2+} oscillations requires Ca^{2+} influx through SOCs. This is concluded from inhibition of the oscillations by removal of extracellular Ca^{2+} and by knockdown of STIM1 (Fig. 4). STIM1 is the sensor of the ER Ca^{2+} content that clusters in response to depletion of ER Ca^{2+} and activates all type of SOCs (31, 39).

The sustained RANKL-induced Ca^{2+} oscillations lead to activation of NFATc1 and osteoclast differentiation (16, 40) to mediate bone remodeling. The crucial physiological roles of the RANKL-induced and activated ROS pathway in osteoclastogenesis and bone remodeling is demonstrated by the marked reduction in bone density observed in the PrxII$^{-/-}$ mouse (Fig. 1). Strikingly, BMMs from PrxII$^{-/-}$ mice showed higher steady-state ROS levels than their WT counterpart and displayed autonomous Ca^{2+} oscillations in the absence of RANKL stimulation. These BMMs are expected to lead to increased osteoclast differentiation and thus reduced bone density. Indeed, scavenging ROS markedly reduced RANKL-induced osteoclastogenesis (Fig. 5*E*).

In summary, the RANK/RANKL-mediated osteoclastogenesis and bone remodeling are complex processes that involve activation of several signaling pathways. RANKL recruits TRAF6 to activate NF-κB and the JNK pathways (13–15) and activates c-Fos and AP-1 (16), all of which are required for the induction of NFATc1 (41–43) (Fig. 6). Once induced, NFATc1 is activated by dephosphorylation that is mediated by the Ca^{2+}-activated phosphatase calcineurin. The present studies identified a ROS-generating pathway that is induced by RANKL to evoke Ca^{2+} oscillations, which start ~24 h after RANKL stimulation and last for more than 72 h, probably until completion of osteoclastogenesis and bone remodeling. The ROS pathway is recognized to play a role in an increasing number of physiological functions (44–46). Manipulation of this pathway may offer a target for treatment of bone-related diseases, such as osteoporosis and osteomalacia. At the same time, consideration of the altered ROS pathway for treatment of other diseases must take into account the critical role of the ROS in RANKL-mediated signaling and bone metabolism.

Acknowledgment—We thank Dr. Dae Yul Yu for sharing Prx II$^{-/-}$ mice.

REFERENCES

1. Rodan, G. A., and Martin, T. J. (2000) *Science* **289,** 1508–1514
2. Takayanagi, H., Ogasawara, K., Hida, S., Chiba, T., Murata, S., Sato, K., Takaoka, A., Yokochi, T., Oda, H., Tanaka, K., Nakamura, K., and Taniguchi, T. (2000) *Nature* **408,** 600–605
3. Ducy, P., Schinke, T., and Karsenty, G. (2000) *Science* **289,** 1501–1504
4. Teitelbaum, S. L. (2000) *Science* **289,** 1504–1508
5. Suda, T., Takahashi, N., and Martin, T. J. (1992) *Endocr. Rev.* **13,** 66–80
6. Udagawa, N., Takahashi, N., Akatsu, T., Tanaka, H., Sasaki, T., Nishihara, T., Koga, T., Martin, T. J., and Suda, T. (1990) *Proc. Natl. Acad. Sci. U.S.A.* **87,** 7260–7264
7. Anderson, D. M., Maraskovsky, E., Billingsley, W. L., Dougall, W. C., Tom-

etsko, M. E., Roux, E. R., Teepe, M. C., DuBose, R. F., Cosman, D., and Galibert, L. (1997) *Nature* **390,** 175–179
8. Hsu, H., Lacey, D. L., Dunstan, C. R., Solovyev, I., Colombero, A., Timms, E., Tan, H. L., Elliott, G., Kelley, M. J., Sarosi, I., Wang, L., Xia, X. Z., Elliott, R., Chiu, L., Black, T., Scully, S., Capparelli, C., Morony, S., Shimamoto, G., Bass, M. B., and Boyle, W. J. (1999) *Proc. Natl. Acad. Sci. U.S.A.* **96,** 3540–3545
9. Kong, Y. Y., Yoshida, H., Sarosi, I., Tan, H. L., Timms, E., Capparelli, C., Morony, S., Oliveira-dos-Santos, A. J., Van, G., Itie, A., Khoo, W., Wakeham, A., Dunstan, C. R., Lacey, D. L., Mak, T. W., Boyle, W. J., and Penninger, J. M. (1999) *Nature* **397,** 315–323
10. Matsumoto, M., Sudo, T., Saito, T., Osada, H., and Tsujimoto, M. (2000) *J. Biol. Chem.* **275,** 31155–31161
11. Yasuda, H., Shima, N., Nakagawa, N., Yamaguchi, K., Kinosaki, M., Mochizuki, S., Tomoyasu, A., Yano, K., Goto, M., Murakami, A., Tsuda, E., Morinaga, T., Higashio, K., Udagawa, N., Takahashi, N., and Suda, T. (1998) *Proc. Natl. Acad. Sci. U.S.A.* **95,** 3597–3602
12. Li, J., Sarosi, I., Yan, X. Q., Morony, S., Capparelli, C., Tan, H. L., McCabe, S., Elliott, R., Scully, S., Van, G., Kaufman, S., Juan, S. C., Sun, Y., Tarpley, J., Martin, L., Christensen, K., McCabe, J., Kostenuik, P., Hsu, H., Fletcher, F., Dunstan, C. R., Lacey, D. L., and Boyle, W. J. (2000) *Proc. Natl. Acad. Sci. U.S.A.* **97,** 1566–1571
13. Kobayashi, N., Kadono, Y., Naito, A., Matsumoto, K., Yamamoto, T., Tanaka, S., and Inoue, J. (2001) *EMBO J.* **20,** 1271–1280
14. Naito, A., Azuma, S., Tanaka, S., Miyazaki, T., Takaki, S., Takatsu, K., Nakao, K., Nakamura, K., Katsuki, M., Yamamoto, T., and Inoue, J. (1999) *Genes Cells* **4,** 353–362
15. Wong, B. R., Josien, R., Lee, S. Y., Vologodskaia, M., Steinman, R. M., and Choi, Y. (1998) *J. Biol. Chem.* **273,** 28355–28359
16. Takayanagi, H., Kim, S., Koga, T., Nishina, H., Isshiki, M., Yoshida, H., Saiura, A., Isobe, M., Yokochi, T., Inoue, J., Wagner, E. F., Mak, T. W., Kodama, T., and Taniguchi, T. (2002) *Dev. Cell* **3,** 889–901
17. Berridge, M. J., Bootman, M. D., and Lipp, P. (1998) *Nature* **395,** 645–648
18. Koga, T., Inui, M., Inoue, K., Kim, S., Suematsu, A., Kobayashi, E., Iwata, T., Ohnishi, H., Matozaki, T., Kodama, T., Taniguchi, T., Takayanagi, H., and Takai, T. (2004) *Nature* **428,** 758–763
19. Shinohara, M., Koga, T., Okamoto, K., Sakaguchi, S., Arai, K., Yasuda, H., Takai, T., Kodama, T., Morio, T., Geha, R. S., Kitamura, D., Kurosaki, T., Ellmeier, W., and Takayanagi, H. (2008) *Cell* **132,** 794–806
20. Harris, M. L., Schiller, H. J., Reilly, P. M., Donowitz, M., Grisham, M. B., and Bulkley, G. B. (1992) *Pharmacol. Ther.* **53,** 375–408
21. Choi, M. H., Lee, I. K., Kim, G. W., Kim, B. U., Han, Y. H., Yu, D. Y., Park, H. S., Kim, K. Y., Lee, J. S., Choi, C., Bae, Y. S., Lee, B. I., Rhee, S. G., and Kang, S. W. (2005) *Nature* **435,** 347–353
22. Mayingi, J., Hélary, G., Noirclere, F., Bacroix, B., and Migonney, V. (2007) *Conf. Proc. IEEE Eng. Med. Biol. Soc.* **2007,** 5119–5122
23. Marks, S. C., Jr., Lundmark, C., Christersson, C., Wurtz, T., Odgren, P. R., Seifert, M. F., Mackay, C. A., Mason-Savas, A., and Popoff, S. N. (2000) *Int. J. Dev. Biol.* **44,** 309–316
24. Ramanadham, S., Yarasheski, K. E., Silva, M. J., Wohltmann, M., Novack, D. V., Christiansen, B., Tu, X., Zhang, S., Lei, X., and Turk, J. (2008) *Am. J. Pathol.* **172,** 868–881
25. Roos, J., DiGregorio, P. J., Yeromin, A. V., Ohlsen, K., Lioudyno, M., Zhang, S., Safrina, O., Kozak, J. A., Wagner, S. L., Cahalan, M. D., Veliçelebi, G., and Stauderman, K. A. (2005) *J. Cell Biol.* **169,** 435–445
26. Park, H. S., Lee, S. H., Park, D., Lee, J. S., Ryu, S. H., Lee, W. J., Rhee, S. G., and Bae, Y. S. (2004) *Mol. Cell. Biol.* **24,** 4384–4394
27. Kraft, R., Grimm, C., Grosse, K., Hoffmann, A., Sauerbruch, S., Kettenmann, H., Schultz, G., and Harteneck, C. (2004) *Am. J. Physiol. Cell Physiol.* **286,** C129–C137
28. Thyagarajan, B., Poteser, M., Romanin, C., Kahr, H., Zhu, M. X., and Groschner, K. (2001) *J. Biol. Chem.* **276,** 48149–48158
29. Kiselyov, K., Wang, X., Shin, D. M., Zang, W., and Muallem, S. (2006) *Cell Calcium* **40,** 451–459
30. Parekh, A. B., and Putney, J. W., Jr. (2005) *Physiol. Rev.* **85,** 757–810
31. Huang, G. N., Zeng, W., Kim, J. Y., Yuan, J. P., Han, L., Muallem, S., and Worley, P. F. (2006) *Nat. Cell Biol.* **8,** 1003–1010
32. Gwack, Y., Feske, S., Srikanth, S., Hogan, P. G., and Rao, A. (2007) *Cell Calcium* **42,** 145–156
33. Wu, M. M., Luik, R. M., and Lewis, R. S. (2007) *Cell Calcium* **42,** 163–172
34. Lee, N. K., Choi, Y. G., Baik, J. Y., Han, S. Y., Jeong, D. W., Bae, Y. S., Kim, N., and Lee, S. Y. (2005) *Blood* **106,** 852–859
35. Arai, F., Miyamoto, T., Ohneda, O., Inada, T., Sudo, T., Brasel, K., Miyata, T., Anderson, D. M., and Suda, T. (1999) *J. Exp. Med.* **190,** 1741–1754
36. Bodmer, J. L., Schneider, P., and Tschopp, J. (2002) *Trends Biochem. Sci.* **27,** 19–26
37. Zorov, D. B., Juhaszova, M., and Sollott, S. J. (2006) *Biochim. Biophys. Acta.* **1757,** 509–517
38. Lee, S. B., Bae, I. H., Bae, Y. S., and Um, H. D. (2006) *J. Biol. Chem.* **281,** 36228–36235
39. Worley, P. F., Zeng, W., Huang, G. N., Yuan, J. P., Kim, J. Y., Lee, M. G., and Muallem, S. (2007) *Cell Calcium* **42,** 205–211
40. Takayanagi, H. (2007) *Ann. N.Y. Acad. Sci.* **1116,** 227–237
41. Asagiri, M., Sato, K., Usami, T., Ochi, S., Nishina, H., Yoshida, H., Morita, I., Wagner, E. F., Mak, T. W., Serfling, E., and Takayanagi, H. (2005) *J. Exp. Med.* **202,** 1261–1269
42. Asagiri, M., and Takayanagi, H. (2007) *Bone* **40,** 251–264
43. Takayanagi, H. (2005) *J. Mol. Med.* **83,** 170–179
44. Dröge, W. (2002) *Physiol. Rev.* **82,** 47–95
45. Pignatelli, P., Pulcinelli, F. M., Lenti, L., Gazzaniga, P. P., and Violi, F. (1998) *Blood* **91,** 484–490
46. Varela, D., Simon, F., Riveros, A., Jørgensen, F., and Stutzin, A. (2004) *J. Biol. Chem.* **279,** 13301–13304